EFFECT OF FIBER LENGTH ON TENSILE AND AE PROPERTIES OF GLASS FIBER/POLYPROPYLENE INJECTION MOLDINGS

T. Morii and N. Jumonji
Department of Materials Science and Engineering, Shonan Institute of Technology
1-1-25 Tsujido-Nishikaigan, Fujisawa, Kanagawa 251-8511, Japan
morii@mate.shonan-it.ac.jp

H. Hamada
Division of Advanced Fibro-Science, Graduate School, Kyoto Institute of Technology
Matsugasaki, Sakyo-ku, Kyoto 606-8585, Japan
hhamada@kit.ac.jp

SUMMARY

This study dealt with effect of fibre length on tensile and AE properties of glass fibre filled PP. Short or long fibre filled PPs were moulded and tensile test was conducted with AE monitoring by dual transducers with resonant frequency of 140kHz and 1MHz. From AE results the effect of fibre length on fracture process was clarified.

Keywords: Polypropylene, Short fibre, Long fibre, Acoustic emission

INTRODUCTION

Polypropylene (PP) has a good balance of price, processibility and physical properties, and nowadays it becomes one of the important materials in various industries such as automotive and electrical industries. However, the mechanical properties of PP (which is one of the conventional thermoplastics) are not so high compared with various kinds of engineering plastics. Therefore PP reinforced by glass fibre has been widely used especially in automotive industry. In automotive industry weight saving is one of the key issues for environmental aspects to develop new cars, and the higher performance of glass fibre reinforced PP (GF/PP) has been demanded by automotive industry, etc. One of the solutions to achieve higher performance of GF/PP is to use longer glass fibre as reinforcement. In injection moulding of standard GF/PP the fibre length after moulding is less than 1mm (less than critical fibre length) and it is difficult to make it longer in the conventional compounding and injection moulding process. In order to overcome this difficulty, the long fibre reinforced polypropylene has been focused. The long fibre reinforced materials such as Glass Mat Thermoplastic (GMT) and long fibre thermoplastics (LFT) injection moulding pellets prepared by wire coating, cross-head extrusion, or thermoplastic pultrusion techniques have recently received much attention [1-8]. In particular, the LFT pellets for injection moulding can give the composites with many significantly enhanced properties in comparison with the conventional short-fibre pellets [9, 10].

In order to understand the effect of fibre length on the mechanical properties the fracture process and mode should be focused during mechanical loading. One of the suitable methodologies to directly monitor the fracture process is acoustic emission (AE) [11-14]. AE can monitor the fracture progress quantitatively in real-time, and many information can be obtained by AE characteristics. Usually AE characteristics was often discussed by the amplitude in order to clarify the fracture mode, however, it was reported that only focusing the amplitude could not clarify the fracture mode [15, 16]. From this reason, we proposed the dual AE transducer methodology. In the dual AE transducer methodology 2 types of transducer with the different resonant frequency were applied in order to discuss the matrix dominant and fibre dominant fractures [17].

From these backgrounds, this study discussed the effect of fibre length on mechanical properties and AE characteristics of short and long glass fibre reinforced polypropylene injection mouldings. AE was monitored by the dual AE transducer system in order to discuss the matrix dominant and fibre dominant fractures.

MATERIALS

Materials used were 4 kinds of glass fibre reinforced polypropylene (PP) summarized in Table 1. Two types of pellets were prepared; one was conventional pellet containing 20wt% of short glass fibre, and the other was long glass fibre type (LFT) pellet which was prepared by pultrusion process. In this process glass fibres were aligned to pultruding direction, and melt PP was coated during the pultrusion process. The length of this pellet was 7mm and fibre weight fraction was 40wt%. In this pellet fibre length was equal to the pellet length. By using these materials 4 kinds of pellets were prepared as listed in Table 1. L20 pellet was the mixture of L40 pellet and neat PP pellet to reduce the fibre content. S40 pellet was prepared by compounding of L40 pellet by extruder and re-pelletized. By using these pellets 4 types of dumbbell-shaped specimens, L40, L20, S40 and S20, were prepared by injection moulding. Usually the specially designated screw is used for injection moulding of LFT pellet to remain the length of glass fibre long. In this paper, however, the conventional type screw was applied for injection moulding of the specimens. The remained lengths of glass fibre after moulding were 1.6mm for L40 and L20 and 0.5mm for S40 and S20.

EXPERIMENTAL PROCEDURE

In order to discuss the effect of fibre length on mechanical properties, static tensile test was performed. Static tensile test was performed under a constant cross-head speed of 1mm/min with 120mm gage length under a room temperature by Instron type universal testing machine (Autograph AG-50KNI, Shimadzu Corp., Japan). During the tensile test AE was monitored by the 7600 series AE instrument (NF Corp., Japan). Here, the dual AE transducer methodology was applied for AE monitoring. AE transducers with the resonant frequency of 140kHz (AE-901S, NF Corp., Japan) and 1MHz (AE-905US, NF Corp., Japan) were installed onto the specimen as shown in Figure 1. The transducer with the resonant frequency of 140kHz was sensitive to matrix dominant fracture and that with the resonant frequency of 1MHz was sensitive to the fibre dominant fracture [17]. AE was monitored with the gain of 40dB and the threshold was 100mV to avoid the inclusion of noise.

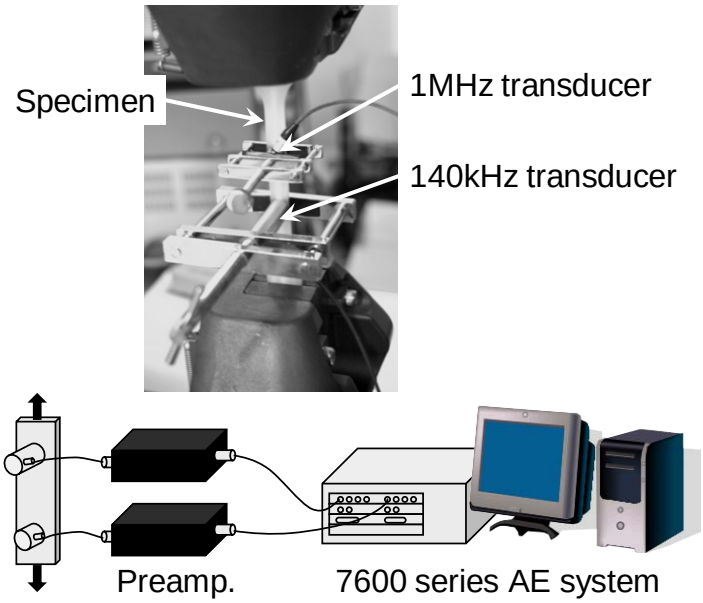

Figure 1 Experimental set-up for AE monitoring during tensile test.

After tensile test the interfacial shear strengths were calculated by following the Kelly-Tyson's formula [18]. The fractured portion was cut from the specimen after tensile test and it was burned out in the electrical furnace under the temperature of 600°C for 4 hours. After burning the remained glass fibres were taken out and they were observed by optical microscope in order to obtain the distribution of fibre length. The interfacial shear strength was calculated by

$$\sigma_{comp}{}^{*} = F\left\{\sum_{l_i > l_c}\left(1-\frac{l_c}{2l_i}\right)V_i\sigma_f{}^{*}+\frac{1}{2}\sum_{l_j<l_c}\left(\frac{l_j\tau_i}{d}\right)V_j\right\}+\sigma_m{}^{*}\left(1-V_f\right) \quad (1)$$

where σ_{comp}* was tensile strength, τ_i was interfacial shear strength, l_c was critical fibre length, l_i was fibre length, d was fibre diameter, σ_m* was matrix strength, σ_f* was fibre strength, V_f was fibre volume fraction, V_i was fibre volume fraction longer than l_c, V_j was fibre volume fraction shorter than l_c and F was coefficient of fibre distribution. Here, F was assumed as 0.85.

EXPERIMENTAL RESULTS AND DISCUSSION

Figure 2 shows the comparison of the tensile strength. In this figure the strength of neat PP was also listed as reference. The strength of L40 was highest among the specimens tested and the long and high content of glass fibre enhanced the strength. The strength of L40 was 25% higher than S40 (same fibre content) and 30% higher than L20 (same fibre length). On the other hand, the strength of L20 was only 5% higher than S20. In low fibre content of LFT the effect of long fibre was little compared with the high fibre content. The interfacial shear strengths were almost the same for L40, L20 and S40. On the other hand, the interfacial shear strength of S20 was higher than the others.

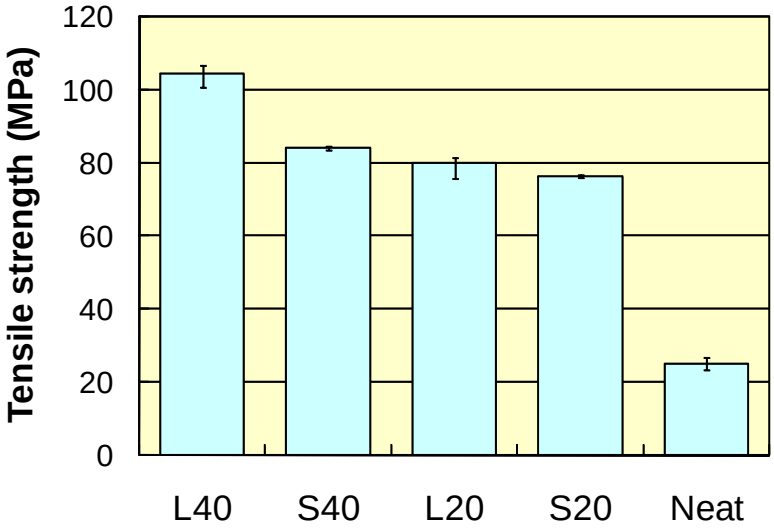

Figure 2 Comparison of tensile strength.

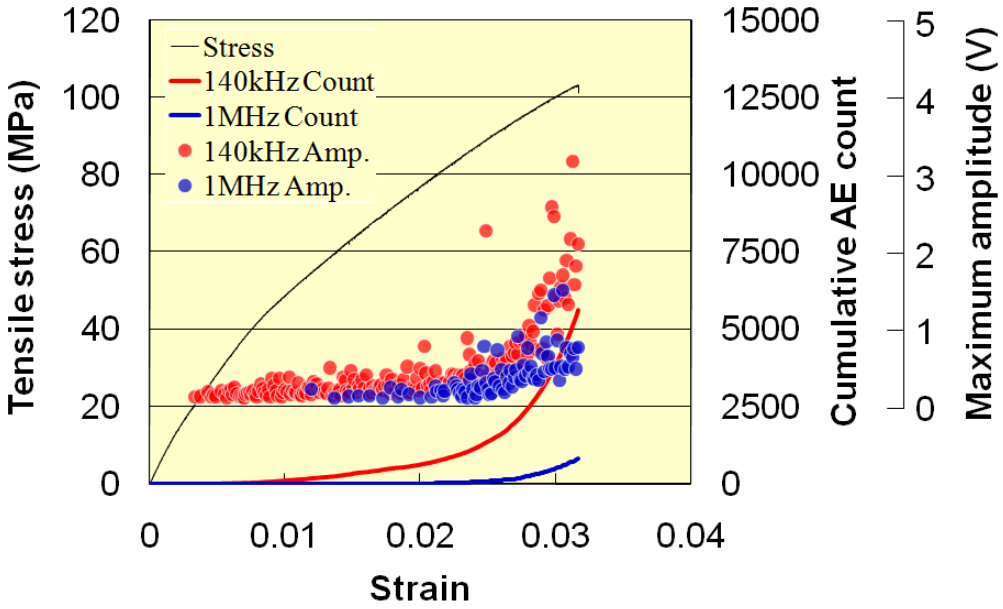

Figure 3 Stress-strain curve and AE characteristics of L40 specimen.

Figures 3 - 6 shows the tensile stress - time curves, cumulative AE count and maximum AE amplitude for L40, L20, S40 and S20 specimens. By comparing L40 and L20 which were the same in fibre length, the trend of cumulative AE count was similar, however, the number of cumulative count of L20 was much higher than L40. In addition, the maximum AE amplitude detected by 1MHz transducer in L20 was much higher than L40. By comparing S40 and S20 the trend of cumulative AE count was similar, and the number of cumulative count of S20 was much higher than S40. The maximum amplitude detected by 1MHz transducer in S20 was higher than S40. These tendencies were the same with L40 and L20. The effect of fibre length on AE characteristics was appeared in the maximum amplitude. The maximum amplitude in

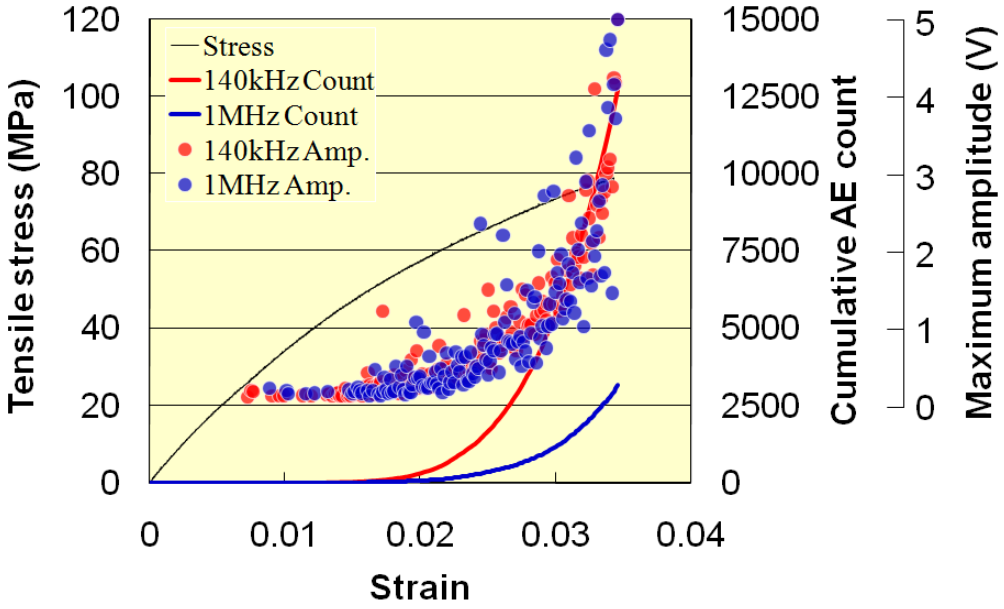

Figure 4 Stress-strain curve and AE characteristics of L20 specimen.

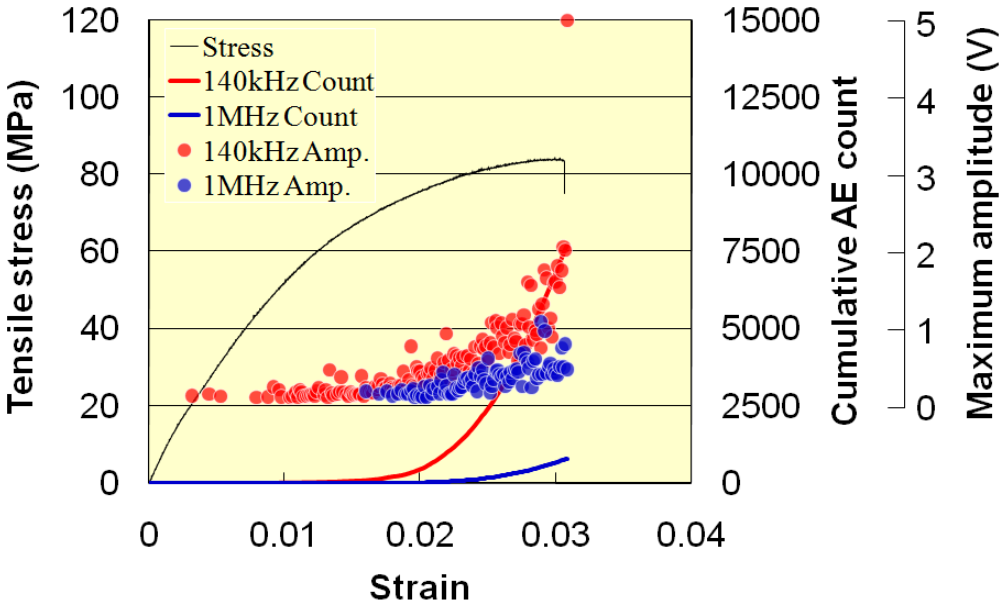

Figure 5 Stress-strain curve and AE characteristics of S40 specimen.

L40 and L20 was higher than those in S40 and S20, respectively. However, the number of cumulative count was almost the same level independent of fibre length.

From the results of AE characteristics the fibre content affected the number of cumulative count and the fibre length affected the maximum amplitude. In the specimen with lower fibre content the applied stress was distributed to all the fibres and the stress supported by each fibre was higher than that in the specimen with higher fibre content. As a result, the AE emitted by fibre breakage in the specimen with lower fibre

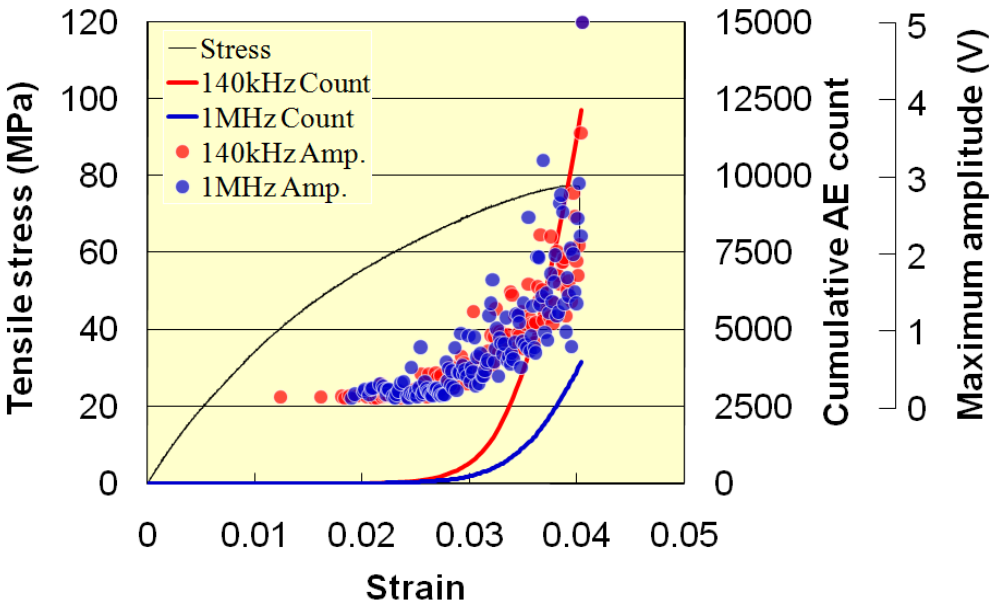

Figure 6 Stress-strain curve and AE characteristics of S20 specimen.

Table 2 Critical fiber length and interfacial shear strength obtained by Kelly-Tyson's analysis.

ID	Critical fiber length (μm)	Interfacial shear strength (MPa)
L40	774	15.8
L20	725	16.9
S40	795	15.4
S20	614	20.0

content had high energy and it resulted in the high amplitude of AE. In the specimen with longer glass fibre each fibre could support high stress without any fracture. As a result, the strain energy released by fibre breakage should be high compared with the specimen with short fibre. Then, the AE energy by fibre breakage in the specimen with longer fibre was higher than that with shorter fibre.

Now the relation between the AE characteristics and the material properties was discussed. Table 2 summarizes the critical fibre length and the interfacial shear strength obtained by the Kelly-Tyson's analysis. The stress where the first AE was detected by 140kHz transducer was about 40MPa independent of the specimen type. As listed in Table 2 the interfacial shear strength of all the specimens were 15 - 20MPa. Generally the first fracture in glass fibre reinforced plastics is caused by the debonding between fibre and matrix, and the bonding strength was closely related to the interfacial strength. Therefore it is considered that the initiation of AE detected by 140kHz transducer

Table 3 Tensile strength and AE initiation stress detected by 1MHz transducer.

ID	Tensile strength (MPa)	AE initiation stress (MPa)
L40	106.1	About 80
L20	78.5	60-70
S40	83.2	60-70
S20	72.0	60-70
PP	23.6	---

corresponded to the initiation of debonding. From this result, the AE initiation stress detected by 140kHz transducer corresponded to the interfacial shear strength. This result meant that interfacial adhesion in glass fibre reinforced injection mouldings might be evaluated by AE and this method was much easier than the Kelly-Tyson's analysis.

Here, the relation between the AE detected by 1MHz transducer and the tensile strength was focused. Table 3 summarizes the tensile strength and the stress at the AE initiation detected by 1MHz transducer. The tensile strength of L40 was much higher than the others and the strengths of L20, S40 and S20 were almost the same level. In the same manner the AE initiation stress detected by 1MHz transducer was about 80MPa in L40 and was about 60-70MPa in L20, S40 and S20. This meant that the order of the AE initiation stress corresponded to the order of the tensile strength. The AE detected by 1MHz transducer was caused by the fibre breakage. The strength of the fibre reinforced plastics depended on the fibre breakage because the broken fibre could not support the applied stress effectively. Therefore AE initiation of 1MHz transducer should correspond to the tensile strength. This suggested that AE monitoring by 1MHz transducer could predict the final rupture of fibre reinforced plastics.

CONCLUSION

This study dealt with the effect of fibre length on AE characteristics of glass fibre reinforced PP injection mouldings. Short and long fibre reinforced PP was moulded by injection moulding, and static tensile tests were conducted with AE monitoring. In AE monitoring, dual transducer system with resonant frequency of 140kHz and 1MHz was adopted. The length of glass fibre affected maximum AE amplitude. The longer fibre induced the AE signals with high amplitude because the stress supported by long fibre was high. The fibre content affected to the number of cumulative count. In the lower content of fibre the applied stress concentrated to a few numbers of fibres and the stress supported by each fibre was high compared at the same applied stress. Eventually many micro fractures occurred and it induced the high cumulative count. The AE initiation stress detected by 140kHz showed same trend with the interfacial shear strength. Therefore the efficiency of interfacial adhesion can be checked by AE monitoring by 140kHz transducer. On the other hand, the AE initiation stress detected by 1MHz corresponded to the tensile strength, and by using this data it might be possible to understand final rupture process.

References

1. J. L. Thomason and M. A. Vlug, Composites, 27A, 477 (1996).
2. J. L. Thomason, M. A. Vlug, G. Schipper and H. G. L. T. Krikor, Composites, 27A, 1075 (1996).
3. J. L. Thomason and M. A. Vlug, Composites, 28A, 277 (1997).
4. J. Karger-Kocsis, Polym. Compos., 21, 514 (2000).
5. A. C. Long, C. E. Wilks and C. D. Rudd, Compos. Sci. Technol., 61, 1591 (2001).
6. N-J. Lee and J. Jang, Compos. Sci. Technol., 60, 209 (2000).
7. K. Waschitschek, A. Kech and J. C. Christiansen, Composites: Part A, 33, 735 (2002).
8. J. L. Thomason, Composites: Part A, 33, 1641 (2002).
9. J. L. Thomason, Composites: Part A, 36, 995 (2005).
10. J. L. Thomason, Composites: Part A, 38, 210 (2007).
11. M. R'Mili, M. Moevus and N. Godin, Compos. Sci. Technol., 68, 1800 (2008).
12. J-M.Park, P-G. Kim, J-H. Jang, Z. Wang, B-S Hwang and K. L. DeVries, Composites: Part B, 39, 1042 (2008).
13. J-M.Park, S. T. Quang, B-S Hwang and K. L. DeVries, Compos. Sci. Technol., 66, 2686 (2006).
14. C. R. Ramirez-Jimenez, N. Papadakis, N. Reynolds, T. H. Gan, P. Purnell and M. Pharaoh, Compos. Sci. Technol., 64, 1819 (2004).
15. M. Faudree, E. Baer, A. Hiltner and J. Collister, J. Compos. Mater., 22, 1170 (1988).
16. C. Kau, A. Hiltner, E. Baer and L. Huber, J. Reinf. Plast. Compos., 8, 18 (1989).
17. T. Morii, N. Jumonji, T. Fujita and T. Horie, Proc. of the 10th Japan International SAMPE Symp. Exhibit., CD-ROM SIT-3-4-1 (2007).
18. A. Kelly and W. R. V. Tyson, J. Mech. Phys. Solids, 13, 329 (1965)